104 (2025) 105176

Contents lists available at ScienceDirect

Poultry Science

journal homepage: www.elsevier.com/locate/psj

Full-Length Article

Adenosine deaminase promotes goose astrovirus genotype II replication in GEF cells

Saimin Zhai [a], Ruixue Li [a], Keying Liu [a], Huichao Gao [a], Xia Yang [a,c], Jun Zhao [a], Xiaozhan Zhang [b], Zeng Wang [a,c,d,*]

[a] College of Veterinary Medicine, Henan Agricultural University, Zhengzhou 450046, China
[b] College of Veterinary Medicine, Henan University of Animal Husbandry and Economy, Zhengzhou 450046, China
[c] Ministry of Education Key Laboratory for Animal Pathogens and Biosafety, Zhengzhou 450046, China
[d] Key Laboratory of Quality and Safety Control of Poultry Products, Ministry of Agriculture and Rural Affairs, Zhengzhou 450046, China

ARTICLE INFO

Keywords:
GAstV-II
ADA
Cap protein
Positive regulation
Interaction

ABSTRACT

Goose astrovirus genotype II (**GAstV-II**), the causative agent of visceral and joint gout in goslings, has been widespread in China since 2016 and resulted in considerable economic losses to waterfowl industry. As an important enzyme involved in purine metabolism and uricogenesis, adenosine deaminase (***ADA***) is reported to be upregulated via GAstV infection. However, knowledge about the regulatory role of ADA played during virus replication is still limited. In the present work, goose ADA (***gADA***) was firstly cloned from goose embryo fibroblasts (**GEF**) and phylogenetic analysis showed that it was highly homologous with duck *ADA*, sharing 96.6 % identity in nucleotide sequences. Moreover, GAstV-II infection promoted the production of *gADA* but did not change its cellular distribution pattern, which was evenly dispersed in the cytoplasm and nucleus. Further results demonstrated that ectopic expression of *gADA* significantly enhanced viral capsid protein expression and virus loads in GEF cells. Conversely, knockdown of *gADA* by siRNA played the opposite role in virus replication. Notably, *gADA* could directly interact with viral capsid protein, particularly with its C-terminal domain. Our data elucidated the regulatory role of *gADA* during GAstV-II infection, thereby laying a solid foundation to further explore its pathogenesis.

Introduction

Goose astrovirus (**GAstV**), belonging to genus *Avastrovirus* of family *astroviridae*, is a single-stranded positive-sense RNA virus with a star-like protrusion on the surface (Shen et al., 2022). The polyadenylated genome is approximately 7.2 kb in length and consists of a 5′-untranslated region (**5′-UTR**), three open reading frames (**ORF**1a, ORF1b, and ORF2), and a 3′-UTR. Thereinto, ORF1a and ORF1b encode non-structural proteins, such as RNA dependent RNA polymerase (**RdRp**), serine protease motif (**Pro**), and nuclear localization signal (**NLS**), which mainly affect the replication and transcription of viral RNA. The capsid (***cap***) protein is synthesized from ORF2, and its N-terminal region is more conserved across all astroviruses whereas the C-terminal counterpart shows high sequence variability. Structurally, *cap* protein contains four domains, including inner core (**S**), outer core (**P1**), spike (**P2**), and acidic domain. Thereinto, acidic domain is thought to be as a binding site for cell receptor during infection (Méndez, et al., 2007), and P2 is responsible for activating host immune response (Arias and DuBois, 2017; Zhang, et al., 2022a). Based on ORF2 sequence, GAstV could be divided into two genotypes, GAstV-I and GAstV-II. Sequence alignment shows that the genome-wide similarity between them is 57.9 %, with that of ORF2 even as low as 42.6 % (Huang, et al., 2021). Until now, GAstV-II has become the predominant strain that circulating in most goose raising provinces in China. Goslings aged under 15 days are vulnerable to GAstV-II and the mortality rate ranges from 20 % to 50 % (Xu, et al., 2023). GAstV-II mainly causes joint and visceral gout in goslings, with the clinical symptoms of depression, weight loss, white feces, joint swelling, and lameness (Chen, et al., 2024). Notably, GAstV-II has been reported in goose embryos, Cherry Valley ducklings, and Muscovy ducklings, suggesting the vertical transmission and cross-species barriers (Chen, et al., 2020, 2021; Wei, et al., 2020). Additionally, GAstV-I is often found co-infection with GAstV-II, further highlighting the importance of virus surveillance and the development of disease control methods (Wang, et al., 2022). It is

* Corresponding author at: College of Veterinary Medicine, Henan Agricultural University, Zhengzhou 450046, China.
E-mail address: wzzxz20140105@126.com (Z. Wang).

https://doi.org/10.1016/j.psj.2025.105176
Received 13 February 2025; Accepted 15 April 2025
Available online 17 April 2025

reported that the incidence rate of GAstV-II could be as high as 80 %, with the mortality rate ranging from 15 % to 30 %. The virus infection greatly threats the development of goose industry in China, with the economic losses have exceeded $10 million (Wang, et al., 2021).

Gout is the most common chronic disease caused by monosodium urate (**MSU**) crystals depositing on the surface of visceral organs and in the joint cavities. The risk of developing gout is positively correlated with the concentrations of serum uric acid (**SUA**) (Dalbeth, et al., 2019). SUA is an intermediate product of purine metabolism and finally excreted as urate through kidney (around two-thirds) and feces (around one-thirds) (Keenan, 2020; Mandal and Mount, 2015). Adenine and guanine from the damaged and dead cells are endogenous purines, and the exogenous ones are those formed in liver and intestinal tract from high protein diets (Choi, et al., 2004). Once the balance of purine intake and output is disrupted, the possibility of developing gout will be highly increased. Generally, there are two ways to increase the level of SUA. One is some risk factors disturb purine metabolic process and cause a great deal of SUA accumulation, with the amount far exceeding discharge capacity. The other is SUA retention caused by kidney dysfunction (Wu, et al., 2022). Therefore, gout could be either a nutrition metabolic disease or a contagious condition.

Purines are essential elements for building DNA and RNA, and purine metabolism is a complex process that involved in its biosynthesis, interconversion, and degradation (Moriwaki, et al., 1999). Disorders of purine metabolism are closely related with diseases induced by hyperuricemia since uric acid is the final product of purine catabolism (So and Thorens, 2010; Zhang, et al., 2022b). Adenosine deaminase (***ADA***) is a crucial enzyme in purine metabolism that catalyzes the conversion of adenosine and deoxyadenosine to inosine and deoxyinosine, which will be eventually converted into SUA (Alfaqih, et al., 2024). Studies have indicated a positive correlation between the production of SUA and the level of *ADA*. Specifically, inhibition of *ADA* could remarkably suppress SUA expression, consequently leading to the alleviation of clinical gout symptoms in rat models (Qian, et al., 2023; Sun, et al., 2022). Similarly, Wu et al. found that goose ADA (***gADA***) activity and mRNA level in liver was increased during GAstV-II replication (Wu, et al., 2020), indicating GAstV-II could hijack purine metabolism via influencing *gADA* expression. However, the exact role of *gADA* during virus infection remains unknown. In this study, therefore, we first cloned *gADA* and described its regulatory roles during GAstV-II infection.

Materials and methods

Virus and cell

GAstV-II HNXX-6/China/2020 strain (GenBank: MW592379) was isolated from week goose embryo from Henan province and preserved in our laboratory. 11-day-old healthy Sanhua goose embryos cultured in Dulbecco's modified Eagle's Medium (Hyclone, USA) supplemented with 10 % fetal bovine serum (Cellmax, China) were used to generate primary goose embryo fibroblasts (**GEF**). Only GAstV-II-negative cells were allowed to be used for further study.

Plasmid construction

Total RNA extracted from GEF cells were reversely transcribed into cDNA with oligo dT, and *gADA* was amplified by using specific primers. After being purified, the amplicons were homologously recombined with linearized pCAGGS-HA vector to construct plasmids pCAGGS-HA-gADA. For truncated *cap* protein, cDNA derived from total RNA extracted from HNXX-6/China/2020 served as template to amplify three fragments of *cap* protein, namely *cap* (1-256aa), *cap* (257-406aa), and *cap* (407-665aa), which were finally ligated into linearized p3 × flag-cmv10 vector to generate respective recombinant plasmids. Primers used in this study were shown in Table 1.

Antibody preparation and purification

200 μg pCAGGS-HA-gADA was intramuscularly injected into the leg of a New Zealand White rabbit at day 1, 14, and 28. After final immunization, the cardiac blood collected from the anesthetized animal was used to separate serum. Subsequently, the antibody was preliminarily purified as follows. The serum was centrifuged at 3000 rpm for 10 min to remove fibrin clots and debris. Saturated ammonium sulfate was then gradually added to a final concentration of 50 %. Following incubation at 4 °C for 1 h, the pellet was dialyzed against PBS to remove residual ammonium sulfate.

Bioinformatic analyses

The sequence of *gADA* and its counterparts of different animals obtained from GenBank were aligned with MegAlign program in DNAstar software package. Subsequently, MEGA 7.0 was used to construct the phylogenetic tree based on the neighbor-joining method with a boot strap of 1000 repetitions.

Indirect immunofluorescence assay (IFA)

GEF cells were mock-infected or infected with HNXX-6/China/2020 at MOI of 0.1 for 12, 24, 36, and 48 h. The cells were then fixed with 4 % paraformaldehyde and permeabilized by 0.1 % Triton X-100 in phosphate buffered saline (**PBS**) at room temperature for 30 min.

Table 1
Primers used for plasmid construction and identification.

Gene	Purpose	Sequence (5′–3′)[1]	Length (bp)
gADA	clone	Forward gattacgctCCTGCCATCGCGGGGGACC Reverse attaagatctTCACGATGCATTGGGCACC	873
gADA	qRT-PCR	Forward ATCAAGGAGGCAGTGTATCTCCTG Reverse GTCATCGGTGTTTATCGAATAGTTAG	221
cap	qRT-PCR	Forward TATTGAGGAATTGCGAGAGGAC Reverse GTAGTTGAGCCATGCTTGTTCTC	288
cap(1-256)	clone	Forward cttgcggccgcgGCAGACAGGGCGGTGGC Reverse tctcagctgacTCACCCTGGTTTTGGACCATAGTTC	768
cap(257-406)	clone	Forward cttgcggccgcgCTCTCACTTATGACCAGTGAAACA Reverse tctcagctgacTCAACCTTGTCCAGTTGTATTCACAT	450
cap(407-665)	clone	Forward cttgcggccgcgCAGGTTACTCCCTCGCTTGTGTAC Reverse tctcagctgacAGAGGTCTTGAGCGAGACAGCTAG	723
GAPDH	qRT-PCR	Forward TATGACTCTACTCATGGCCACTTCAAG Reverse GATGATGACACGCTTAGCACCACC	218
sigADA-1	knockdown	GGUGAACAACUUCAUCCGG	-
sigADA-2	knockdown	UUCACUAUGCUGUAAUCCG	-
sigADA-3	knockdown	UUAUCGAAUAGUUAGCCCG	-

[1] The lower letters were designed for homologously recombined with pCAGGS-HA vector linearized by *EcoR I* and *Nhe I*.

Subsequently, the cells were blocked with 5 % BSA at 37 °C for 1 h, incubated with rabbit anti-gADA antibody (dilution 1:100), and successively with FITC-conjugated Affinipure Goat Anti-Rabbit IgG(H + L) (Proteintech, China) (dilution 1:2000). After being washed with PBS for three times, the cells were stained with 4′,6-diamidino-2-phenylindole (**DAPI**) (Solarbio, China) at room temperature for 15 min. And the location and intensity of green fluorescence were observed via fluorescence microscope.

Quantitative real-time PCR (qRT-PCR)

Total RNA of GEF cells were reversely transcribed into cDNA, which was taking as the template to amplify *gADA* or GAstV-II *cap* by using specific primers shown in Table 1. The expression was normalized to the housekeeping gene GAPDH. The experiments were replicated for three times and the results were calculated via the comparative CT ($2^{-\triangle\triangle CT}$) method (Schmittgen and Livak, 2008).

Co-immunoprecipitation (Co-IP)

The indicated plasmids were transfected into GEF cells cultured in 6-well plate by using Lipofectamine 6000 (Beyotime, China). 48 h later, the cells were washed with chilled PBS and then lysed with IP lysis buffer (Beyotime, China) for 30 min on ice. After centrifuging at 10,000 rpm for 10 min at 4 °C, the supernatants were incubated with mouse anti-HA monoclonal antibody (**mAb**) (Proteintech, China) (dilution 1:2000) at 4 °C overnight, and then mixed with protein G-agarose beads for further 8 h at 4 °C. The beads were then washed three times with PBS, the bound proteins were separated by SDS-PAGE and detected by western blot.

Western blot

GEF cells harvested at various time points were lysed on ice with radioimmunoprecipitation assay (RIPA) (Beyotime, China) buffer for 30 min.The supernatants collected after being centrifuged at 10, 000 rpm for 10 min at 4 °C were subjected to 10 % SDS-PAGE. Based on the different types of proteins, rabbit anti-*gADA* polyclonal antibody (**pAb**) (dilution 1:100), rabbit anti-*cap* pAb (dilution 1:200), rabbit anti-*GAPDH* mAb (ABclonal, USA) (dilution 1:1000), mouse anti-flag mAb (Proteintech, China) (dilution 1:2000), and mouse anti-HA mAb (dilution 1:2000) were used as the primary antibodies, and horseradish peroxidase (**HRP**)-conjugated goat anti-rabbit IgG (H + L) (Proteintech, China) (dilution 1:5000) and anti-mouse IgG (H + L) (Proteintech, China) (dilution 1:5000) were used as the secondary antibodies. The proteins were finally visualized by using chemiluminescence ECL kit, after being washed for three times.

Knockdown of gADA via siRNA

siRNAs targeting *gADA* and a non-targeting control (**siNC**) were designed and synthesized (shown in Table 1). To validate the specificity, potential homology between siRNAs and other genes was analyzed via bioinformatics analysis, and those with more than 16 consecutive base matches to other genes were avoided. Secondly, online software siRNAscan was used to predict the off-target risk. Moreover, three siRNAs targeting different regions of *gADA* were designed to make sure the consistent silencing phenotype. To evaluate the knockdown efficiency, GEF cells seeded in 6-well plate were transfected with siRNAs by using Lipofectamine RNAiMax (Invitrogen, USA). The cells were collected at 24 h for qRT-PCR and 48 h for western blot to detect the knockdown efficiency.

Measurement of GAstV-II growth in GEF cells

GEF cells cultured in 96-well plate were infected with serially 10-fold diluted virus and incubated at 37 °C with 5 % CO_2. 72 h later, viral titers were calculated according to the Reed-Muench method as previously described (Ma, et al., 2023).

Protein structure prediction

gADA protein was constructed by using AlphaFold3 program with basic method setting. The structure of GAstV-II *cap* protein was constructed through homology modeling, utilizing turkey astrovirus capsid protein (PDB: 3TS3) as the template, with the aid of MOE2015 program.

Molecular docking

Binding complexes between *gADA* and GAstV-II *cap* were predicted via HDOCK server (http://hdock.phys.hust.edu.cn/). The top 10 output models were provided with docking scores and confidence scores for the evaluation of their reliability. When the docking score was below −200 and the confidence score was above 0.7, the two molecules would be very likely to bind. Subsequently, the result ranked first was visualized by means of PyMOL software.

Statistical analysis

The data are presented as means and standard deviations (**SD**). Statistical significance between groups was determined by ANOVA with post-hoc Tukey's test by using GraphPad Prism 7.0 software.

Results

Identification and sequence analysis of gADA

To determine the function of *gADA* during GAstV-II infection, its full length ORF was first cloned from the cDNA of GEF cells. The identified *gADA* sequence consisted of 873 nucleotides encoding a protein of 290 amino acids. Accordingly, a phylogenic tree was constructed and *gADA* was found to be clustered in the bird clade (Fig. 1). Further analysis showed that *gADA* exhibited the highest homology with duck ADA (***dADA***) (up to 96.6 %), followed by chicken ADA (***cADA***) (up to 89.7 %)

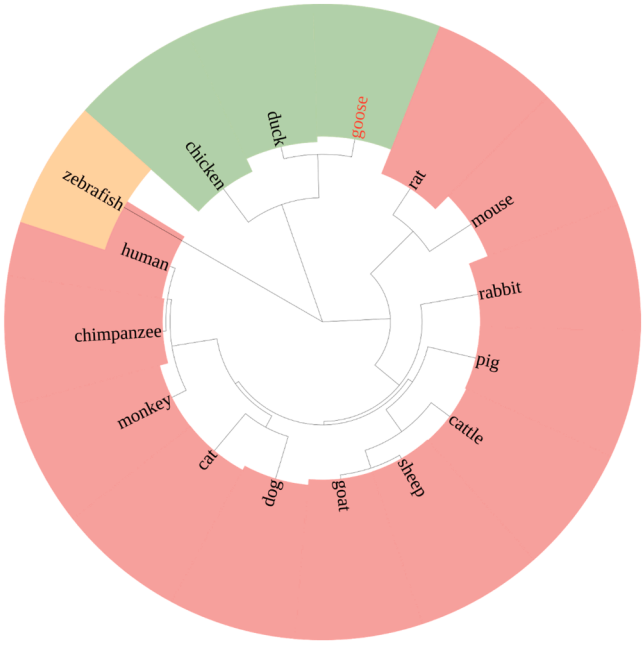

Fig. 1. Phylogenetic analysis of gADA. A neighbor-joining tree was constructed by using MEGA 7.0 software based on the nucleotide sequences of gADA homologs from different species.

in gene sequence. Similarly, the amino acid sequence of *gADA* had an identity of 95.2 % with *dADA* and 89.6 % with *cADA*, indicating that *gADA* had a relatively strong homology with those of avian species.

GAstV-II infection promotes the expression of gADA

GEF cells infected or non-infected with HNXX-6/China/2020 were fixed at indicated time points and IFA was performed to detect the subcellular localization of *gADA*. Results showed that green fluorescence was evenly distributed between the cytoplasm and nucleus in physiological GEF cells, even with the similar distribution pattern in the infected ones (Fig. 2A). Notably, the quantity and intensity of green fluorescence was gradually increased along with infection, suggesting the production of *gADA* might be positively upregulated. To further explore the expression kinetics of *gADA* during virus infection, infected GEF cells were harvested at indicated time points to perform qRT-PCR and western blot. As shown in Fig. 2B and 2C, the production of *gADA* was significantly improved at mRNA and protein level in infected GEF cells at 24, 36, and 48 h post-infection (**hpi**) compared to those in the uninfected ones. These data indicated that GAstV-II promoted *gADA* expression without affecting its subcellular localization.

gADA stimulates GAstV-II replication in vitro

To explore the specific function of *gADA* during GAstV-II infection, GEF cells transfected with pCAGGS-HA-gADA or pCAGGS-HA vector were infected with HNXX-6/China/2020 at an MOI of 0.1. Cells and supernatants were separately harvested to detect virus replication via qRT-PCR, western blot, and 50 % tissue culture infective dose (**$TCID_{50}$**). Results demonstrated that the production of *cap* was sharply increased at both mRNA level (Fig. 3A) and protein level (Fig. 3B) in *gADA* overexpression group, especially at 36 hpi. Further, virus titers in this group reached 2.22, 4.04, and 4.63 $Log_{10}(TCID_{50}/100\ \mu L)$ at 24, 36, and 48 h, respectively, and they were significantly higher than those in the control group, which were 1.59, 2.68, and 3.66 $Log_{10}(TCID_{50}/100\ \mu L)$, respectively (Fig. 3C). These data suggested that *gADA* played a positive role in regulating GAstV-II replication in GEF cells.

Interfering gADA limits GAstV-II replication

To further confirm the regulatory effect of *gADA* during GAstV-II infection, we examined virus replication in GEF cells with *gADA* knockdown at different time points. GEF cells were firstly transfected with siRNA or siNC and the interference effect was evaluated via qRT-PCR (Fig. 4A) and western blot (Fig. 4B). Data demonstrated that the knockdown efficiency of all the three siRNAs reached above 50 %, with that of siRNA2 approximately 70 %, and thereby, it was deployed in the further study. Subsequently, GEF cells transfected with siRNA2 or siNC were infected with HNXX-6/China/2020 at an MOI of 0.1, and the supernatants and cells were collected to investigate virus replication. As shown in Fig. 4C and Fig. 4D, the expression of cap was significantly decreased at both mRNA level and protein level in *gADA* knockdown cells, compared to those in the control ones. Similarly, virus loads in *gADA* knockdown group were 1.09 and 2.08 $Log_{10}(TCID_{50}/100\ \mu L)$ at 24 and 36 hpi, respectively, which were far below than those in the counterpart group of 1.23 and 3.28 $Log_{10}(TCID_{50}/100\ \mu L)$ (Fig. 4E). These data further confirmed that *gADA* was positively correlated with the GAstV-II replication in GEF cells.

gADA interacts with GAstV-II cap protein

Given the positive regulation of GAstV-II replication by *gADA*, we sought to investigate whether *gADA* could bind to *cap* protein. Firstly, we performed molecular docking to predict the binding possibility between the two proteins. As shown in Fig. 5A, all the docking scores of the top ten binding complexes were below −200 and the confidence scores were above 0.7, suggesting the two proteins were highly likely to interact with each other. Additionally, the visualized structure of the first ranked result also clearly showed the interaction between the two proteins. Subsequently, we further evaluated their interaction via Co-IP assays. GEF cells were transfected with either HA-tagged *gADA* or an empty vector, and subsequently infected with HNXX-6/China/2020 at MOI of 0.1. Cell lysates were subjected to immunoprecipitation with a mouse anti-HA mAb, followed by western blot with a rabbit anti-*cap* pAb. As shown in Fig. 5B, a clear interaction between *gADA* and *cap* protein was observed, as the *cap* protein was coimmunoprecipitated with HA-tagged *gADA* but not the HA empty vector, confirming *gADA* as a binding partner of the viral *cap* protein. To further define the crucial domain of cap protein essential for its interaction with *gADA*, we constructed three plasmids expressing the inner core, outer core, or spike domain fused with flag tag at the N-terminus (Fig. 5C). By conducting Co-IP assays with *gADA* as the bait protein in GEF cells transfected with the indicated combination of plasmids, *cap* (407-665aa) was detectable in cells expressing HA-*gADA* (Fig. 5D), suggesting that spike domain was crucial for cap binding with *gADA*.

Discussion

As a multifunctional protein, *ADA* can 1) catalyze the hydrolytic deamination of adenosine and 2′-deoxyadenosine to inosine and 2′ deoxyinosine, respectively (Jiang, et al., 1997); 2) bind extracellularly to adenosine receptors to maintain adenosine homeostasis (Gracia, et al., 2013); 3) act as a positive regulator to potentiate the generation of effector, memory, and regulatory CD4+ *T* cells (Martinez-Navio, et al., 2011). Since purine metabolism disorder is the etiology of gout and GAstV-II is the main causative pathogen of visceral and joint gout in goslings, exploring the regulatory role of the critical enzyme *gADA* in GAstV-II caused gout is particularly important. Here, we firstly performed phylogenetic analysis and found that *gADA* shared the highest homology with *dADA*. IFA showed that *gADA* was uniformly resident in the cytoplasm and nucleus, even without any change during GAstV-II infection. Previous study shows that humans contain three types of *ADA* isoenzymes, *ADA1, ADA1+CP*, and *ADA2*, and they mainly reside in the cytoplasm and also appear on the cell surface, but rarely distribute in nucleus (Gao, et al., 2022; Ginés, et al., 2002). Whether species and sequence variations contributing to the distribution differences and whether there is any isoform(s) of *gADA* still need to be further illustrated.

It has been well described that acute increase of extracellular adenosine concentration in response to inflammation could induce the expression of *ADA* (Eltzschig, et al., 2006; Jedrzejewska, et al., 2023). Subsequently, *ADA* decreases the level of adenosine by converting it to inosine to alleviate inflammatory response (Kaljas, et al., 2017). Similarly, GAstV has been reported to promote an inflammatory reaction and also increased the expression of *gADA* (Liu, et al., 2023; Wu, Xu, Lv and Bao, 2020). Given this, we further investigated the function of *gADA* during virus replication. Our findings revealed that *gADA* expression was significantly upregulated in GAstV-II-infected GEF cells. Moreover, down-regulation of *gADA* expression suppressed GAstV-II replication, whereas overexpression of *gADA* exerted an enhancing effect. Mechanistically, *gADA* could directly interact with *cap* protein. Studies report that ORF2 encodes the capsid precursor protein with the molecular mass of approximately 90 kDa (***VP90***), which is further cleaved intracellularly at the acidic domain to yield mature *VP70* (Méndez, et al., 2004). Since acidic domain acts as the ligand to interact with cell receptor, the processing of *VP90* to *VP70* has been correlated with virus release from cell surface. *VP70* is then extracellularly processed via trypsin to finally produce *VP34, VP27*, and *VP25* (Méndez, et al., 2002). *VP34* contains the complete inner core, which forms the core domain of the virus, and *VP27* plus *VP25* contain the complete spike domain, which forms the protruding region of the virus and plays a central role in viral infection by mediating receptor binding (Ghosh, et al., 2024), facilitating cell

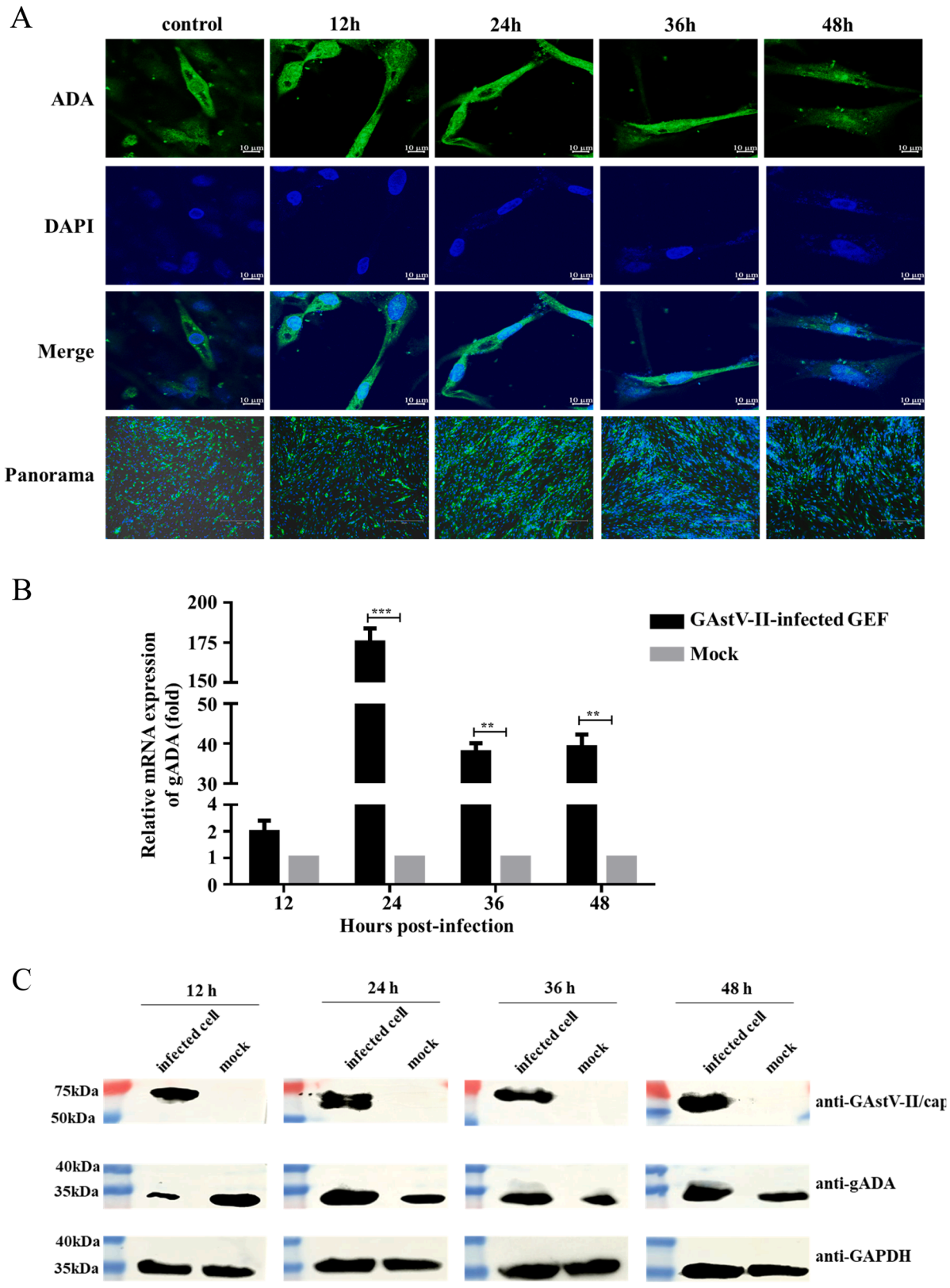

Fig. 2. gADA expression pattern during GAstV-II infection. GEF cells were challenged with HNXX-6/China/2020 at an MOI of 0.1, and samples were harvested at 12, 24, 36, and 48 hpi for further analysis. (A) The subcellular distribution of endogenous gADA in infected- and noninfected-cells were detected by using home-made rabbit anti-gADA polyclonal antibody and FITC-conjugated goat anti-rabbit IgG($H + L$). DAPI, cell nucleus; Merge, superposition scene of green and blue fluorescence; Panorama, a panoramic view with reduced magnification. (B) Total RNA were reversely transcribed into cDNA, and qRT-PCR was performed to detect the mRNA production of gADA. (C) Collected cells were lysed and subjected to western blot to detect the production of gADA at protein level. Data were presented as mean ± SD of three independent experiments and the statistics analysis was performed by ANOVA. **, $P < 0.01$, and ***, $P < 0.005$.

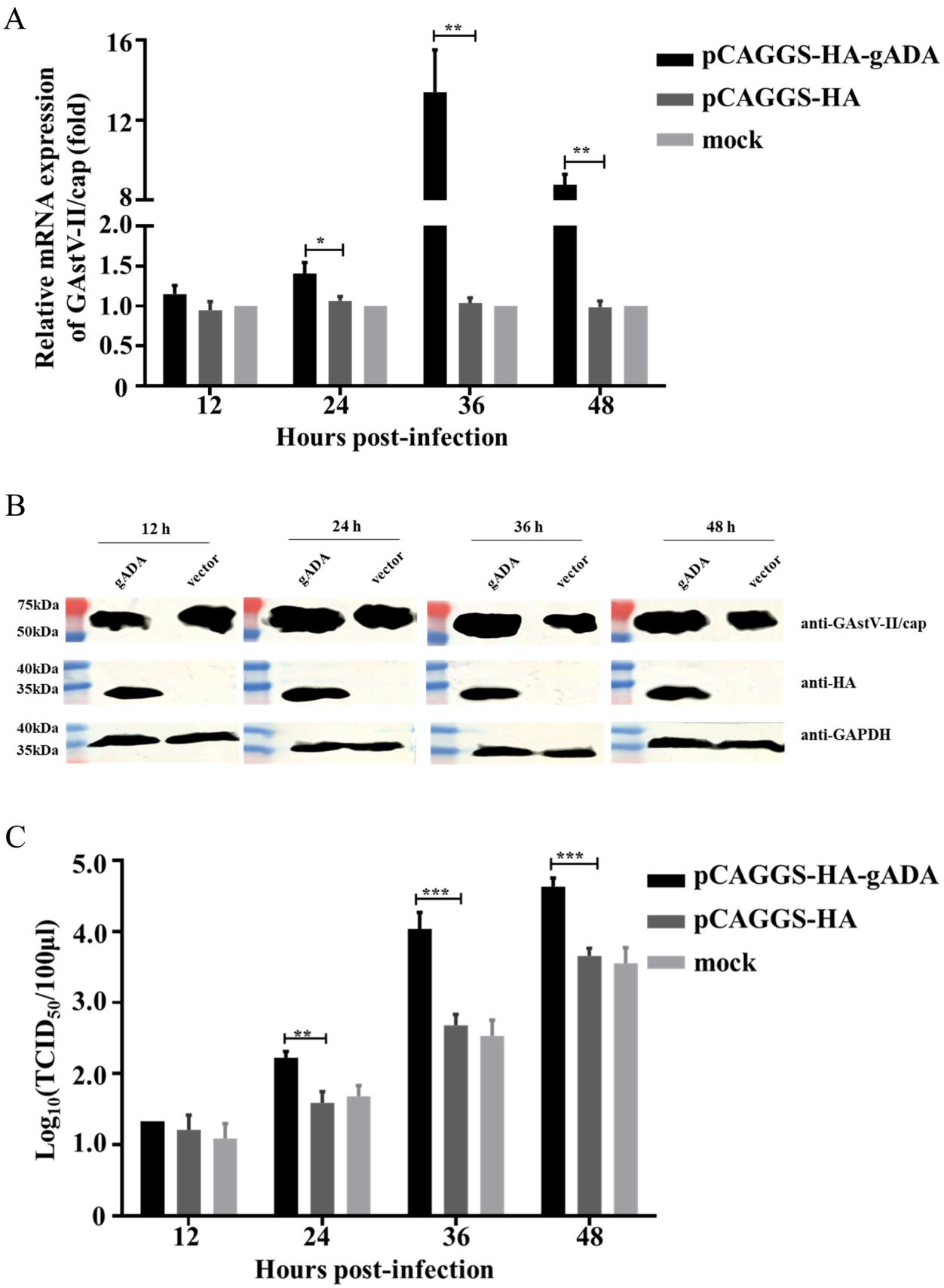

Fig. 3. Effect of gADA overexpression on GAstV-II replication. GEF cells transfected with pCAGGS-HA-gADA, pCAGGS-HA, or untreated were infected with HNXX-6/China/2020 at an MOI of 0.1, and samples were collected at 12, 24, 36, and 48 hpi for further analysis. cDNA and cell lysates were subjected to qRT-PCR (A) and western blot (B) to detect the expression level of cap. Cell supernatants were titrated to calculate $TCID_{50}$ to evaluate virus growth kinetics (C). *, $P < 0.05$, **, $P < 0.01$, and ***, $P < 0.005$.

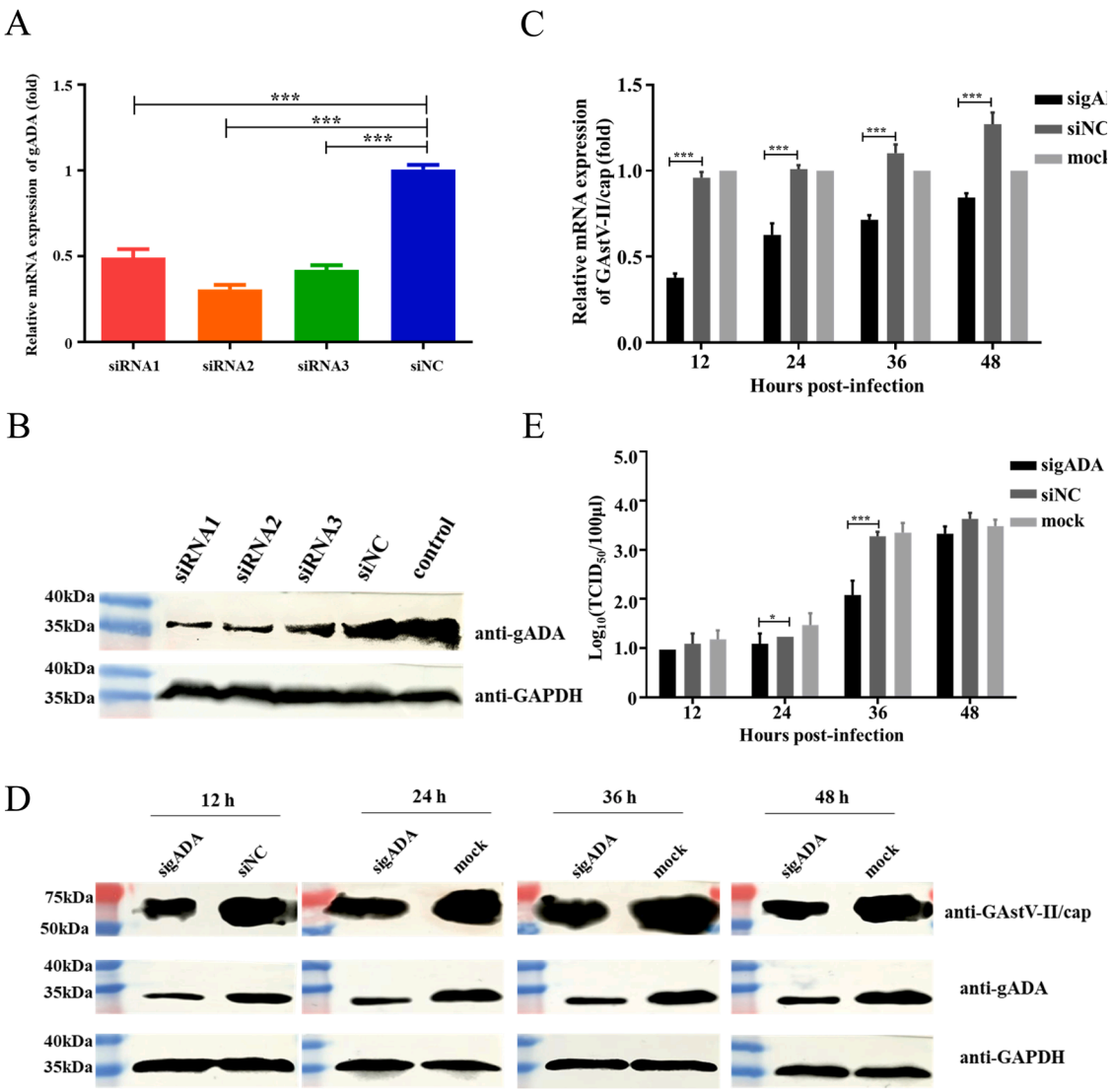

Fig. 4. Effect of gADA knockdown on GAstV-II infection. GEF cells administered with siRNA or siNC were collected and qRT-PCR (A) and western blot (B) were performed to evaluate the knockdown effect. GEF cells transfected with siRNA2, siNC, or untreated were infected with HNXX-6/China/2020 at an MOI of 0.1. Cells and supernatants were collected at indicated time points and analyzed with qRT-PCR (C), western blot (D), or virus titration (E), respectively. *, $P < 0.05$, and ***, $P < 0.005$.

entry (Arias and DuBois, 2017), and modulating host immune responses (Lanning, et al., 2023). Here, we found that *gADA* served as a binding partner of *cap* protein via its spike domain. Given its critical roles in virus infection, further study should explore the effects of interaction between *gADA* and *cap* protein on aspects, such as invasion, assembly, and regulation of host immune response, so as to elucidate the mechanism by which *gADA* promotes GAstV-II replication. Moreover, further study should focus on verifying whether *gADA* can facilitate GAstV-II infection in susceptible goslings, since GEF cells could not fully simulate the complex *in vivo* environment.

Previous data demonstrates that there are five active site residues for human ADA (***hADA***), Cys^{262}, His^{17}, His^{214}, His^{238}, and Glu^{217}, essential for its catalytic activity. Thereinto, mutant with replacement Cys^{262} retains around 40 % of wild-type activity, however, mutants with the other four replacements almost loss the enzyme activity (Bhaumik, et al., 1993). Sequence alignment indicates that His^{145}, His^{169}, and Glu^{148} of *gADA* are probably the active sites. However, whether *gADA* depended on its catalytic activity to drive pro-viral effect remains unclear. Therefore, further studies should be focused on expressing *gADA* with enzymatic activity, identifying its critical active sites, and then exploring whether the catalytic activity of *gADA* has a specific impact on GAstV-II replication. Simultaneously, analyzing the 3D structure of the protein complex between *gADA* and *cap*, and elucidating their specific interactive sites and modes, will be helpful to determine whether *gADA* exerts its positively regulatory role relying on its spatial structure. Apart from being as an indispensable enzyme participated in production of uric acid, *ADA* has been reported to be deeply involved in immune system activities (Antonioli, et al., 2012). *ADA* deficiency causes an accumulation of toxic purine degradation by-products, which resulting in adenosine deaminase severe combined immunodeficiency (**ADA-SCID**) (Passos, et al., 2018). Study reports that GAstV-II infection causes lymphocyte apoptosis and proinflammatory phenotype in macrophages (Ding, et al., 2024). However, the immunomodulatory function of *gADA* remains unknown and whether the increased *gADA* during GAstV-II infection exerts host immune response also needs further investigation.

Collectively, these results provide insights to the function of *gADA* by indicating for the first time that *gADA* is a positive factor in GAstV-II infection, which lays a solid foundation for further development of new antiviral strategies.

A

Rank	Docking score	Confidence score	Ligand rmsd (Å)
1	-265.39	0.9095	44.52
2	-259.89	0.9001	71.74
3	-251.89	0.8847	69.86
4	-247.44	0.8753	68.94
5	-242.41	0.8639	70.35
6	-238.15	0.8536	78.57
7	-236.81	0.8502	37
8	-234.47	0.8441	62.03
9	-229.18	0.8297	72.79
10	-228.7	0.8284	83.67

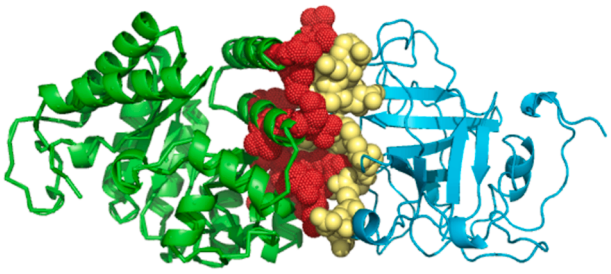

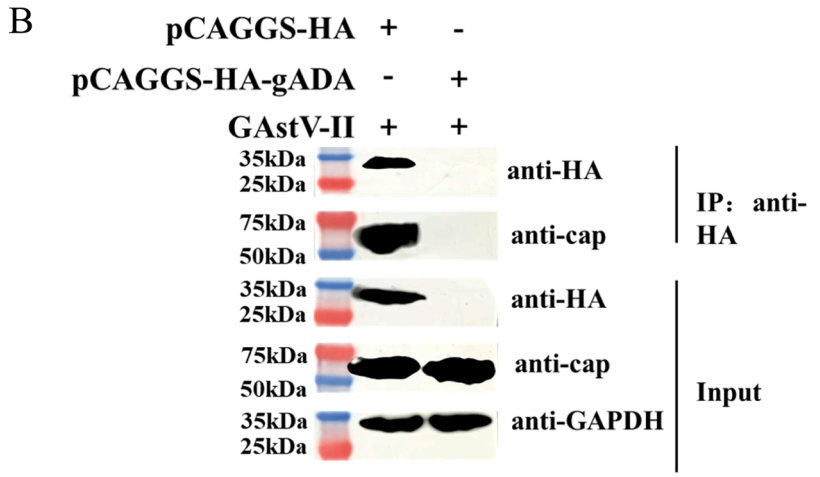

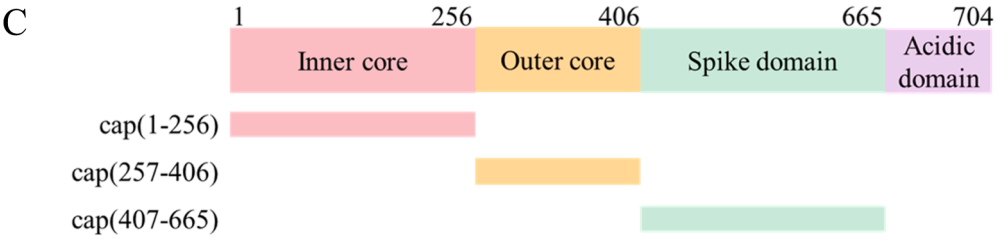

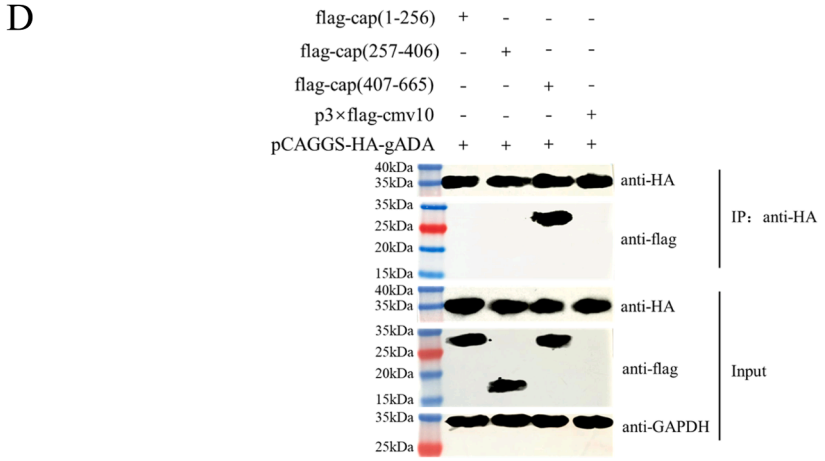

Fig. 5. gADA interacts with the cap protein of GAstV-II. (A) The list of top 10 predicted binding models and the visualized structure of the first ranked result. Protein structure of gADA and GAstV-II cap was individually constructed and then molecular docking was performed via HDOCK server to predict the binding possibility between the two proteins. The model ranked first was then visualized via PyMOL software. (B) GEF cells transfected with HA-gADA were infected with HNXX-6/China/2020 at an MOI of 0.1. At 48 h post-infection, cell lysates were immunoprecipitated with a mouse anti-HA mAb. The bound protein was subjected into western blot with a rabbit anti-cap pAb and mouse anti-HA mAb. (C) Schematic representation of flag-tagged cap structural domains. (D) GEF cells were co-transfected with plasmid HA-tagged gADA, together with flag, flag-cap (1-256), flag-cap (257-406), or flag-cap (407-665). At 48 h post-transfection, the cell lysates were incubated with mouse anti-HA mAb, and the bound proteins were detected by western blot with mouse anti-flag mAb.

Ethics statement

The research protocols for animal experiments were approved by the Animal Care and Use Committee of Henan Agricultural University (HNND2024030505).

Disclosures

The authors declare no conflict of interest.

Declaration of competing interest

The authors declare that they have no known competing financial interests or personal relationships that could have appeared to influence the work reported in this paper.

Acknowledgement

This work was supported by the Science and Technological Project of Henan Province (242102111016); Program for Science & Technology Innovation Talents in Universities of Henan Province (24HASTIT061); Henan Provincial Excellent Young Scientist Foundation Project (252300421155).

References

Alfaqih, M.A., Ababneh, E., Mhedat, K., Allouh, M.Z., 2024. Vitamin D reduces the activity of adenosine deaminase and oxidative stress in patients with type two diabetes mellitus. Mol. Nutr. Food Res. 68, e2300870. https://doi.org/10.1002/mnfr.202300870.

Antonioli, L., Colucci, R., La Motta, C., Tuccori, M., Awwad, O., Da Settimo, F., Blandizzi, C., Fornai, M., 2012. Adenosine deaminase in the modulation of immune system and its potential as a novel target for treatment of inflammatory disorders. Curr. Drug Targets 13, 842–862. https://doi.org/10.2174/138945012800564095.

Arias, C.F., DuBois, R.M., 2017. The astrovirus capsid: a review. Viruses-Basel 9, 15. https://doi.org/10.3390/v9010015.

Bhaumik, D., Medin, J., Gathy, K., Coleman, M.S., 1993. Mutational analysis of active site residues of human adenosine deaminase. J. Biol. Chem. 268, 5464–5470.

Chen, H., Zhang, B., Yan, M., Diao, Y.X., Tang, Y., 2020. First report of a novel goose astrovirus outbreak in Cherry Valley ducklings in China. Transbound. Emerg. Dis. 67, 1019–1024. https://doi.org/10.1111/tbed.13418.

Chen, L.G., Cui, H., Li, J.Q., Zhang, Y.X., Wang, H., Yang, Y.J., Wang, X.J., Zhang, C., Liu, J.X., 2024. Epidemiological investigation of goose astrovirus in Hebei Province, China, 2019-2021. Microorganisms 12, 990. https://doi.org/10.3390/microorganisms12050990.

Chen, Q.X., Yu, Z.L., Xu, X., Ji, J., Yao, L.G., Kan, Y.C., Bi, Y.Z., Xie, Q.M., 2021. First report of a novel goose astrovirus outbreak in Muscovy ducklings in China. Poult. Sci. 100, 101407. https://doi.org/10.1016/j.psj.2021.101407.

Choi, H.K., Atkinson, K., Karlson, E.W., Willett, W., Curhan, G., 2004. Purine-rich foods, dairy and protein intake, and the risk of gout in men. N.Engl. J. Med. 350, 1093–1103. https://doi.org/10.1056/NEJMoa035700.

Dalbeth, N., Choi, H.K., Joosten, L.A.B., Khanna, P.P., Matsuo, H., Perez-Ruiz, F., Stamp, L.K., 2019. Gout. Nat. Rev. Dis. Primers 5, 69. https://doi.org/10.1038/s41572-019-0115-y.

Ding, R., Xu, H.R., Huang, H., Cao, R.B., Lv, Y.J., 2024. Effects of Goose astrovirus type 2 infection on peripheral blood lymphocyte and macrophage activity. Viral Immunol. 37, 139–148. https://doi.org/10.1089/vim.2023.0098.

Eltzschig, H.K., Faigle, M., Knapp, S., Karhausen, J., Ibla, J., Rosenberger, P., Odegard, K. C., Laussen, P.C., Thompson, L.F., Colgan, S.P., 2006. Endothelial catabolism of extracellular adenosine during hypoxia: the role of surface adenosine deaminase and CD26. Blood 108, 1602–1610. https://doi.org/10.1182/blood-2006-02-001016.

Gao, Z.-W., Yang, L., Liu, C., Wang, X., Guo, W.-T., Zhang, H.-Z., Dong, K., 2022. Distinct roles of adenosine deaminase isoenzymes ADA1 and ADA2: a pan-cancer analysis. Front. Immunol. 13, 903461. https://doi.org/10.3389/fimmu.2022.903461.

Ghosh, A., Delgado-Cunningham, K., López, T., Green, K., Arias, C.F., DuBois, R.M., 2024. Structure and antigenicity of the divergent human astrovirus VA1 capsid spike. PLoS Pathog. 20, e1012028. https://doi.org/10.1371/journal.ppat.1012028.

Ginés, S., Mariño, M., Mallol, J., Canela, E.I., Morimoto, C., Callebaut, C., Hovanessian, A., Casadó, V., Lluis, C., Franco, R., 2002. Regulation of epithelial and lymphocyte cell adhesion by adenosine deaminase-CD26 interaction. Biochem. J. 361, 203–209. https://doi.org/10.1042/0264-021:3610203.

Gracia, E., Farré, D., Cortés, A., Ferrer-Costa, C., Orozco, M., Mallol, J., Lluís, C., Canela, E.I., McCormick, P.J., Franco, R., Fanelli, F., Casadó, V., 2013. The catalytic site structural gate of adenosine deaminase allosterically modulates ligand binding to adenosine receptors. FASEB J. 27, 1048–1061. https://doi.org/10.1096/fj.12-212621.

Huang, H., Ding, R., Chen, Z.Y., Yi, Z.W., Wang, H.Y., Lv, Y.J., Bao, E.D., 2021. Goose nephritic astrovirus infection increases autophagy, destroys intercellular junctions in renal tubular epithelial cells, and damages podocytes in the kidneys of infected goslings. Vet. Microbiol. 263, 109244. https://doi.org/10.1016/j.vetmic.2021.109244.

Jedrzejewska, A., Kawecka, A., Braczko, A., Romanowska-Kocejko, M., Stawarska, K., Deptula, M., Zawrzykraj, M., Franczak, M., Krol, O., Harasim, G., Walczak, I., Pikula, M., Hellmann, M., Kutryb-Zajaç, B., 2023. Changes in adenosine deaminase activity and endothelial dysfunction after mild coronavirus disease-2019. Int. J. Mol. Sci. 24, 13140. https://doi.org/10.3390/Ijms241713140.

Jiang, C., Hong, R., Horowitz, S.D., Kong, X., Hirschhorn, R., 1997. An adenosine deaminase (ADA) allele contains two newly identified deleterious mutations (Y97C and L106V) that interact to abolish enzyme activity. Hum. Mol. Genet. 6, 2271–2278. https://doi.org/10.1093/hmg/6.13.2271.

Kaljas, Y., Liu, C.Q., Skaldin, M., Wu, C.X., Zhou, Q., Lu, Y.N., Aksentijevich, I., Zavialov, A.V., 2017. Human adenosine deaminases ADA1 and ADA2 bind to different subsets of immune cells. Cell. Mol. Life Sci. 74, 555–570. https://doi.org/10.1007/s00018-016-2357-0.

Keenan, R.T., 2020. The biology of urate. Semin. Arthritis Rheum. 50,. https://doi.org/10.1016/j.semarthrit.2020.04.007. S2-S10.

Lanning, S., Pedicino, N., Haley, D.J., Hernandez, S., Cortez, V., DuBois, R.M., 2023. Structure and immunogenicity of the murine astrovirus capsid spike. J. Gen. Virol. 104, 001913. https://doi.org/10.1099/Jgv.0.001913.

Liu, C., Li, L., Dong, J., Zhang, J., Huang, Y., Zhai, Q., Xiang, Y., Jin, J., Huang, X., Wang, G., Sun, M., Liao, M., 2023. Global analysis of gene expression profiles and gout symptoms in goslings infected with goose astrovirus. Vet. Microbiol. 279, 109677. https://doi.org/10.1016/j.vetmic.2023.109677.

Méndez, E., Aguirre-Crespo, G., Zavala, G., Arias, C.F., 2007. Association of the astrovirus structural protein VP90 with membranes plays a role in virus morphogenesis. J. Virol. 81, 10649–10658. https://doi.org/10.1128/Jvi.00785-07.

Méndez, E., Fernández-Luna, T., López, S., Méndez-Toss, M., Arias, C.F., 2002. Proteolytic processing of a serotype 8 human astrovirus ORF2 polyprotein. J. Virol. 76, 7996–8002. https://doi.org/10.1128/Jvi.76.16.7996-8002.2002.

Méndez, E., Salas-Ocampo, E., Arias, C.F., 2004. Caspases mediate processing of the capsid precursor and cell release of human astroviruses. J. Virol. 78, 8601–8608. https://doi.org/10.1128/Jvi.78.16.8601-8608.2004.

Ma, Y.-c., Chen, H.-y., Gao, S.-y., Zhang, X.-z., Li, Y.-t., Yang, X., Zhao, J., Wang, Z., 2023. A novel short transcript isoform of chicken IRF7 negatively regulates interferon-β production. J. Integr. Agr. 22, 2213–2220. https://doi.org/10.1016/j.jia.2022.12.015.

Mandal, A.K., Mount, D.B., 2015. The molecular physiology of uric acid homeostasis. Annu. Rev. Physiol. 77, 323–345. https://doi.org/10.1146/annurev-physiol-021113-170343.

Martinez-Navio, J.M., Casanova, V., Pacheco, R., Naval-Macabuhay, I., Climent, N., Garcia, F., Gatell, J.M., Mallol, J., Gallart, T., Lluis, C., Franco, R., 2011. Adenosine deaminase potentiates the generation of effector, memory, and regulatory CD4+ T cells. J. Leukoc. Biol. 89, 127–136. https://doi.org/10.1189/jlb.1009696.

Moriwaki, Y., Yamamoto, T., Higashino, K., 1999. Enzymes involved in purine metabolism–a review of histochemical localization and functional implications. Histol. Histopathol. 14, 1321–1340. https://doi.org/10.14670/HH-14.1321.

Passos, D.F., Bernardes, V.M., da Silva, J.L.G., Schetinger, M.R.C., Leal, D.B.R., 2018. Adenosine signaling and adenosine deaminase regulation of immune responses: impact on the immunopathogenesis of HIV infection. Purinergic Signal 14, 309–320. https://doi.org/10.1007/s11302-018-9619-2.

Qian, X.W., Jiang, Y., Luo, Y.Y., Jiang, Y.C., 2023. The anti-hyperuricemia and anti-inflammatory effects of atractylodes macrocephala in hyperuricemia and gouty arthritis rat models. Comb. Chem. High T Scr. 26, 950–964. https://doi.org/10.2174/1386207325666220603101540.

Schmittgen, T.D., Livak, K.J., 2008. Analyzing real-time PCR data by the comparative C (T) method. Nat. Protoc. 3, 1101–1108. https://doi.org/10.1038/nprot.2008.73.

Shen, Q.A., Zhuang, Z., Lu, J.A., Qian, L.L., Li, G.Q., Kanton, A.G., Yang, S.X., Wang, X.C., Wang, H.Y., Yin, J., Zhang, W., 2022. Genome analysis of goose-origin astroviruses causing fatal gout in Shanghai, China reveals one of them belonging to a novel type is a recombinant strain. Front. Vet. Sci. 9, 878441. https://doi.org/10.3389/fvets.2022.878441.

So, A., Thorens, B., 2010. Uric acid transport and disease. J. Clin. Invest. 120, 1791–1799. https://doi.org/10.1172/JCI42344.

Sun, X.W., Wen, J., Guan, B.S., Li, J.L., Luo, J.C., Li, J., Wei, M.Y., Qiu, H.B., 2022. Folic acid and zinc improve hyperuricemia by altering the gut microbiota of rats with high-purine diet-induced hyperuricemia. Front. Microbiol. 13, 907952. https://doi.org/10.3389/Fmicb.2022.907952.

Wang, A.P., Zhang, S., Xie, J., Gu, L.L., Wu, S., Wu, Z., Liu, L., Feng, Q., Dong, H.Y., Zhu, S.Y., 2021. Isolation and characterization of a goose astrovirus 1 strain causing fatal gout in goslings, China. Poult. Sci. 100, 101432. https://doi.org/10.1016/j.psj.2021.101432.

Wang, H.Y., Zhu, Y.C., Ye, W.C., Hua, J.G., Chen, L., Ni, Z., Yun, T., Bao, E.D., Zhang, C., 2022. Genomic and epidemiological characteristics provide insights into the phylogeographic spread of goose astrovirus in China. Transbound. Emerg. Dis. 69, E1865–E1876. https://doi.org/10.1111/tbed.14522.

Wei, F., Yang, J., He, D., Diao, Y.X., Tang, Y., 2020. Evidence of vertical transmission of novel astrovirus virus in goose. Vet. Microbiol. 244, 108657. https://doi.org/10.1016/J.Vetmic.2020.108657.

Wu, W.K., Xu, R., Lv, Y.J., Bao, E.D., 2020. Goose astrovirus infection affects uric acid production and excretion in goslings. Poult. Sci. 99, 1967–1974. https://doi.org/10.1016/j.psj.2019.11.064.

Wu, Z.D., Yang, X.K., He, Y.S., Ni, J., Wang, J., Yin, K..J., Huang, J.X., Chen, Y., Feng, Y. T., Wang, P., Pan, H.F., 2022. Environmental factors and risk of gout. Environ. Res. 212, 113377. https://doi.org/10.1016/J.Envres.2022.113377.

Xu, J.Y., Gao, L.G., Zhu, P.D., Chen, S., Chen, Z.X., Yan, Z.Q., Lin, W.C., Yin, L.J., Javed, M.T., Tang, Z.X., Chen, F., 2023. Isolation, identification, and pathogenicity analysis of newly emerging gosling astrovirus in South China. Front. Microbiol. 14, 1112245. https://doi.org/10.3389/Fmicb.2023.1112245.

Zhang, X.Z., Deng, T.W., Song, Y.Z., Liu, J., Jiang, Z.H., Peng, Z.F., Guo, Y.W., Yang, L., Qiao, H.X., Xia, Y..X., Li, X.Z., Wang, Z., Bian, C.Z., 2022a. Identification and genomic characterization of emerging goose astrovirus in central China, 2020. Transbound. Emerg. Dis. 69, 1046–1055. https://doi.org/10.1111/tbed.14060.

Zhang, Y.L., Chen, S.M., Yuan, M., Xu, Y., Xu, H.X., 2022b. Gout and diet: a comprehensive review of mechanisms and management. Nutrients 14, 3525. https://doi.org/10.3390/Nu14173525.